

UC Berkeley

UC Berkeley Previously Published Works

Title

Changes in Four Decades of Near-CONUS Tropical Cyclones in an Ensemble of 12 km Thermodynamic Global Warming Simulations

Permalink

<https://escholarship.org/uc/item/9z1233b4>

Journal

Geophysical Research Letters, 51(18)

ISSN

0094-8276

Authors

Zarzycki, Colin M

Zhang, Tyrone

Jones, Andrew D

et al.

Publication Date

2024-09-28

DOI

10.1029/2024gl110535

Copyright Information

This work is made available under the terms of a Creative Commons Attribution License, available at <https://creativecommons.org/licenses/by/4.0/>

Peer reviewed

Geophysical Research Letters®

RESEARCH LETTER

10.1029/2024GL110535

Key Points:

- Thermodynamic global warming simulations provide a unique large-sample size view into paired counterfactual tropical cyclones
- 12 km simulations indicate future near-United States cyclones will, on average, be wetter, slightly more intense, but similarly sized
- Periods of rapid intensification and weakening indicate increased tropical cyclone intensity variability in warmer climates

Supporting Information:

Supporting Information may be found in the online version of this article.

Correspondence to:

C. M. Zarzycki,
czarzycki@psu.edu

Citation:

Zarzycki, C. M., Zhang, T., Jones, A. D., Rastogi, D., Vahmani, P., & Ullrich, P. A. (2024). Changes in four decades of near-CONUS tropical cyclones in an ensemble of 12 km thermodynamic global warming simulations. *Geophysical Research Letters*, 51, e2024GL110535. <https://doi.org/10.1029/2024GL110535>

Received 4 JUN 2024
Accepted 26 AUG 2024





Author Contributions:

Conceptualization: Colin M. Zarzycki, Andrew D. Jones
Data curation: Andrew D. Jones, Deeksha Rastogi, Pouya Vahmani
Formal analysis: Colin M. Zarzycki, Tyrone Zhang
Funding acquisition: Colin M. Zarzycki, Andrew D. Jones, Paul A. Ullrich
Investigation: Colin M. Zarzycki, Tyrone Zhang
Methodology: Colin M. Zarzycki, Andrew D. Jones, Deeksha Rastogi, Pouya Vahmani
Project administration: Colin M. Zarzycki, Andrew D. Jones, Paul A. Ullrich

© 2024. The Author(s).

This is an open access article under the terms of the [Creative Commons Attribution License](https://creativecommons.org/licenses/by/4.0/), which permits use, distribution and reproduction in any medium, provided the original work is properly cited.

Changes in Four Decades of Near-CONUS Tropical Cyclones in an Ensemble of 12 km Thermodynamic Global Warming Simulations

Colin M. Zarzycki¹ , Tyrone Zhang¹, Andrew D. Jones^{2,3} , Deeksha Rastogi⁴ , Pouya Vahmani² , and Paul A. Ullrich^{5,6}

¹Department of Meteorology and Atmospheric Science, Pennsylvania State University, University Park, PA, USA, ²Climate and Ecosystem Sciences Division, Lawrence Berkeley National Laboratory, Berkeley, CA, USA, ³Energy and Resources Group, University of California, Berkeley, Berkeley, CA, USA, ⁴Computational Sciences and Engineering Division, Oak Ridge National Laboratory, Oak Ridge, TN, USA, ⁵Division of Physical and Life Sciences, Lawrence Livermore National Laboratory, Livermore, CA, USA, ⁶Department of Land, Air and Water Resources, University of California, Davis, Davis, CA, USA

Abstract We evaluate tropical cyclones (TCs) in a set of thermodynamic global warming (TGW) simulations over the continental United States (CONUS). A 12 km simulation forced by ERA5 provides a 40-year historical (1980–2019) control. Four complimentary future scenarios are generated using thermodynamic deltas applied to lateral boundary, interior, and surface forcing. We curate a data set of 4,498 6-hourly TC snapshots in the control and find a corresponding “twin” in each counterfactual, permitting a paired comparison. Warming results in an increase in mean dynamical TC intensity and moisture-related quantities, with the latter being more pronounced. TC inner cores contract slightly but outer storm size remains unchanged. The frequency with which TCs become more intense is only moderately consistent, with snapshots having increased hazards ranging from 50% to 80% depending on warming level. The fractions of TCs undergoing rapid intensification and weakening both increase across all warming simulations, suggesting elevated short-term intensity variability.

Plain Language Summary We examined how tropical cyclones (TCs) near the United States might change due to warmer climates. First, we recreated past weather conditions from 1980 to 2019 using a specialized climate model. Then, we predicted future changes in the same meteorology by modifying the model to include warmer temperatures and running four additional simulations. We tracked and analyzed over 4,000 instances of TCs from the past 40 years, ensuring that these TCs were all matched between all five simulations, and evaluated their changes under future warming conditions. Our findings suggest that TCs will become stronger on average as the world warms, with the most notable increases in TC moisture. Not every TC in our study becomes more intense with warming, however, highlighting the complexity of understanding how extreme weather will change in the future. We found that the chances of a TC rapidly intensifying or suddenly weakening both rise with higher levels of warming. These trends could complicate predictions of TC intensity in the future, presenting additional challenges for forecasting and preparation.

1. Introduction

Tropical cyclones (TCs) cause extensive property damage, economic disruption, and harm to livelihoods. Understanding future TC changes is important to inform preparedness and mitigation strategies, help safeguard vulnerable communities, and reduce deleterious economic impacts (Mendelsohn et al., 2012).

Numerous studies have explored projected future changes in TCs using free-running global climate models (GCMs) (Knutson et al., 2020, and references therein). High-resolution GCMs that permit TCs provide detailed information regarding changes in both frequency and intensity. However, it can be difficult to disentangle the two, and model biases may complicate interpretation. An alternative approach that only explores the impact of thermodynamic changes on existing TCs is the thermodynamical global warming (TGW) approach, sometimes referred to as “imposed warming” or “pseudo-global warming.” Briefly, TGW involves reproducing historical weather, then modifying these simulations with a thermodynamic signal derived from coupled GCMs to predict the same weather events under future climate conditions (Brogli et al., 2023; Schär et al., 1996). This

Resources: Colin M. Zarzycki, Andrew D. Jones, Paul A. Ullrich

Software: Colin M. Zarzycki, Tyrone Zhang, Deeksha Rastogi, Pouya Vahmani, Paul A. Ullrich

Supervision: Colin M. Zarzycki, Andrew D. Jones

Validation: Colin M. Zarzycki

Visualization: Colin M. Zarzycki, Tyrone Zhang

Writing – original draft: Colin M. Zarzycki, Tyrone Zhang

thermodynamic signal is commonly called a “delta” and represents a background anthropogenic warming pattern present in a given climate scenario.

The primary strength of TGW is that it permits the evolution of known events under counterfactual conditions. It effectively asks, “If the same meteorological event occurred under a different thermodynamic environment, how would the event’s evolution change?” This idea is tightly linked with the growing application of storylines for evaluating and communicating climate impacts (Shepherd et al., 2018), which provide event-based assessments describing the physically consistent unfolding of past events and plausible future pathways (Ciullo et al., 2021). TGW’s core weakness is that it is *conditional* on the historical event evolving under highly similar synoptic conditions and, therefore, cannot predict changes in event frequency.

Generally, TGW has been applied to individual TCs or aggregations of hindcasts of storms (e.g., Chen et al., 2020; Chow et al., 2024; Delfino et al., 2023; Lackmann, 2015; Olschewski & Kunstmann, 2024; C. L. Parker et al., 2018; Patricola & Wehner, 2018; Reddy et al., 2021; Reed et al., 2020; Tran et al., 2022, and others). While the results are not identical in each study, the consensus is that perturbing historical TCs results in noticeably higher precipitation rates and storm-total precipitation. More modest increases in storm intensity are generally found, although some studies find little change or even weaker TCs with warming (Wehner et al., 2019). Gutmann et al. (2018) performed a temporally continuous 4 km TGW simulation and looked at 22 TCs over the United States (US) from 2001 to 2013. Under added warming, they found simulated TCs had faster maximum winds, slower translation speeds, lower pressures, and higher precipitation rates, although there was large TC-to-TC variation.

Here, we evaluate five 12 km simulations (one historical, four TGW) over the continental US (CONUS) and compare matching sets of near-coastal TCs. Instead of the more commonly applied approach of performing short hindcasts of individual storms, we perform continuous integrations following a single initialization, similar to Gutmann et al. (2018). In addition to applying model grid spacings finer than current state-of-the-art high-resolution GCMs (Haarsma et al., 2016), this study contains two novelties that have not been previously published, to our knowledge. First, we analyze an ensemble of TGW runs with the same meteorology but varying levels of warming rather than a single control and counterfactual. This permits the exploration of a range of potential outcomes, both in terms of total domain warming as well as the spatial pattern of thermodynamic changes. Second, we evaluate an unprecedented sample size for TCs in a TGW simulation—346 distinct TCs spanning 4,498 6-hourly timesteps—with a large suite of TC metrics. This permits the generation of a large database of high-resolution storylines.

2. Data and Methods

2.1. Model Data

The simulations applied here are described in detail in Jones et al. (2023). To summarize, a 40-year (1980–2019) downscaled CONUS simulation is generated using a 12 km (39 level) configuration of the Weather Research Forecasting Model (WRF, v4.2.1). The grid spacing and horizontal domain were designed to achieve a balance between accurately simulating CONUS extremes and computational expense. Three-hourly European Centre for Medium-Range Weather Forecasts version 5 reanalysis (ERA5) fields were applied as lateral boundary conditions (LBCs). TCs are well-represented in ERA5 (Bourdin et al., 2022), and TCs that form over the open ocean are introduced to the domain via these LBCs. Spectral nudging (SN) was added in the interior of the mesh to further constrain the large-scale meteorology but allow sub-synoptic scales to evolve freely. Daily sea surface temperatures (SSTs) are derived from ERA5 and prescribed as a fixed lower boundary condition. This recreation is referred to as the “historical” run and is schematically shown in Figure 1a.

Four counterfactual climates are then generated by defining two subsets of CMIP6 simulations with higher (“hot”) and lower (“cold”) climate sensitivity (Jones et al., 2023). Climate deltas—differences in variables (here, air temperature, near-surface air temperature, skin temperature, relative humidity, and sea-surface temperature) between a projected climate state and a baseline (present-day) state—are then extracted from CMIP6 and added to the original ERA5 LBCs, SN, and surface forcing. Atmospheric concentrations of greenhouse gases are adjusted accordingly. The simulation is then re-run for a “near” scenario (applying 2020–2059 deltas to recreate 1980–2019) and a “far” scenario (applying 2060–2099 deltas) with both the “hot” and “cold” groupings, resulting in four counterfactuals (Figure 1b). Note, since we apply daily SST from ERA5, surface forcing contains moderate TC cold wakes. Since large-scale deltas are applied to the SST in the counterfactuals, the relative SST cooling

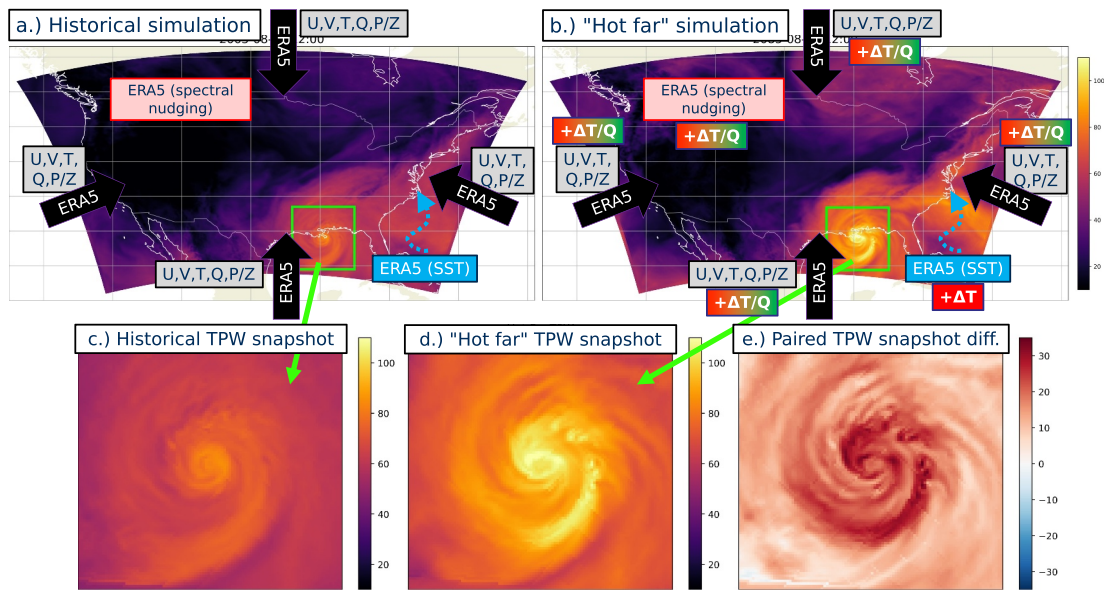


Figure 1. Snapshots of total precipitable water (TPW) at 12Z 29th August 2005 (effective), for the historical (a.) and the “hot far” (b.) simulations over the WRF domain. Warmer colors represent higher TPW values (mm). The green outline in the two panels denotes the snapshot box surrounding Hurricane Katrina used for TC comparison for both simulations (c. and d. show a zoom of this box). Paired differences are computed from these snapshots to quantify how a TC at a given time and location changes in the counterfactual runs (e.).

response to TCs is similar in all simulations. An example is shown in Supporting Information S1 (Figure S1). Because the SSTs are prescribed, this study doesn't include mechanisms that impact TC's influence on the upper ocean, such as changes in thermal or salinity stratification (Balaguru et al., 2016; Huang et al., 2015).

An overview of the permutations is shown in the top rows of Table 1. While we apply the Shared Socioeconomic Pathway (SSP585, Meinshausen et al., 2020) scenario here, we encourage readers to focus on the CONUS warming levels (WLs), also shown in Table 1, rather than the precise scenario. These warming levels represent the domain-averaged realized surface temperature warming of each simulation relative to the historical reference. While the pattern of warming may vary somewhat at the same WL for different scenarios, warming levels remove a large component of emission scenario uncertainty (and associated economic, social, and political behaviors) from the projection (James et al., 2017).

2.2. TC Tracking and Statistics

Tracking TCs here provides a unique challenge. Since the runs are forced with ERA5, the output is effectively a reanalysis. However, because of the weak constraint on small spatial scales, TCs do not necessarily occur in *exactly* their location identified in the historical record. To address this, we use the observational International Best Track Archive for Climate Stewardship (IBTrACS, Knapp et al., 2010) and only keep simulated sea level pressure (SLP) values within 3° of an observed TC's center at a given time. We also ignore any TCs within 8 gridboxes of the model lateral boundaries. We then track the local minimum SLP (simulated TC center) within the valid “patches” using TempestExtremes (Ullrich & Zarzycki, 2017; Ullrich et al., 2021) to allow for a modeled TC offset of up to approximately 330 km from the recorded observation location. This analysis is performed for each simulation to create five sets of trajectories. These trajectory files are then curated so that only TC points detected in every simulation are preserved. That is, we compose a one-to-one correspondence of 346 TCs (4,498 timesteps) that occurred during the 1980–2019 period for each simulation through a series of track trimmings, mergers, and deletions. TC fixes that cannot be credibly detected in all five data sets are ignored. Each of the timesteps (i.e., a specific TC at a specific time and location along its trajectory) is referred to as a TC “snapshot,” which can be directly matched to the same TC snapshot in another simulation. We choose to keep all TCs both pre- and post-landfall. The included TCs are contained in Supporting Information S1 (Tables S1, S2, and Figure S2). Because of this tracking methodology, as well as how the model is forced both by LBCs and SN, we do not

Table 1

Model Configurations (Top, Gray Lines), WLs Over CONUS (Middle, Pink Line), and TC Statistics (Bottom, White Lines)

		Units	Hist.	Cold Near	Hot Near	Cold Far	Hot Far
SSP / RCP				5 / 8.5	5 / 8.5	5 / 8.5	5 / 8.5
GCM Sensitivity				Low	High	Low	High
Time Period			1980–2019	2020–2059	2020–2059	2060–2099	2060–2099
CONUS Warming Level	WL	°C	0	1.6	2.4	3.8	5.7
Sea Surface Temperature (2x2° under center)	SST	°C	26.4	27.6	28.1	29.1	30.3
Min. Sea Level Pressure	MSLP	hPa	1000.5 (969.0)	999.8 (967.3)	999.5 (965.6)	999.3 (964.9)	999.0 (962.6)
Max. 10-m Wind	$u_{10m,x}$	m s ⁻¹	18.4 (36.1)	18.9 (37.3)	19.2 (38.0)	19.5 (38.7)	19.9 (39.9)
Storm Integrated Kinetic Energy	IKE	TJ	29.1 (127.3)	30.2 (130.6)	30.4 (132.9)	31.3 (136.1)	31.5 (135.0)
Max. Total Precipitable Water	TPW _x	mm	68.4 (80.8)	75.4 (89.1)	78.0 (92.5)	84.8 (100.2)	93.0 (111.4)
Max. Precipitation Rate	Prec _x	mm hr ⁻¹	22.9 (52.6)	26.0 (58.9)	27.5 (62.6)	30.1 (67.1)	33.7 (76.1)
Area Precipitation Rate > 10 mm hr ⁻¹	Prec _{area>10}	1000 km ²	9.0 (34.3)	10.8 (39.3)	11.6 (41.4)	13.2 (44.8)	14.6 (49.2)
Radius of 8 m s ⁻¹ 850-hPa Wind	r_8	km	470 (1083)	472 (1081)	470 (1083)	469 (1082)	469 (1083)
Radius of Max. 10-m Wind	RMW	km	148 (34)	140 (32)	143 (32)	140 (29)	141 (29)
6-hourly Sea Level Pressure Variation	dPSL	hPa 6hr ⁻¹	2.0 (5.7)	2.1 (6.4)	2.2 (6.6)	2.3 (7.1)	2.4 (7.8)

Note. For each statistic, the mean of the entire snapshot distribution is on top, with the 95th percentile (5th percentile for MSLP and RMW) shown below in italics. The mean is bolded and underlined if the underlying distribution composing it differs significantly from the historical reference distribution at the 99% confidence level using Welch's *t*-test. The mean is only bolded (underlined) if significant at the 95% (90%) level.

evaluate potential changes in TC translation speed or quantities that may be impacted by changes in TC motion (e.g., latitude of maximum intensity, storm-total rainfall).

Two-dimensional snapshot fields are extracted by specifying a 10°x10° box centered on the tracked TC (Figures 1c–1e). All subsequent analysis computes metrics that are either the snapshot minimum/maximum (e.g., maximum wind) or area integrals (e.g., wind field size). To ensure the simulations are adequate-for-purpose (W. S. Parker, 2011) (i.e., TCs are simulated with reasonable fidelity), the median absolute track error in the historical simulation (relative to IBTrACS) is computed to be 75.2 km, confirming the majority of TC snapshots occur within 1° of their observed counterpart (Table S3 in Supporting Information S1). The median TC minimum SLP (maximum 10-m wind) bias for TCs in the historical run is +2.1 hPa (-3.7 m s⁻¹), indicating simulated TCs are slightly too weak (Figure S3 in Supporting Information S1). This is consistent with numerical models at similar grid spacings (Roberts et al., 2020), although these intensity statistics are improved versus conventional reanalyses (C. M. Zarzycki et al., 2021), likely due to increased resolution. Davis (2018) argues that a grid spacing close to 14 km is necessary for the statistical depiction of intense Atlantic hurricanes that preserves a realistic wind structure. While the grid spacing here is slightly finer, it should be noted that the full spectrum of inner-core TC dynamics, including the representation of deep convection within the eyewall, is not resolved.

3. Results

3.1. Mean Statistics

Table 1 shows the mean statistics for numerous TC-relevant metrics (Table S4 in Supporting Information S1) starting with the MSLP row. The top number in each cell highlights the mean metric value for all 4,498 snapshots for that simulation, while the bottom italicized number represents the 95th percentile for each distribution (5th percentile for MSLP and RMW). Statistical significance is noted by bolded and/or underlined mean values using Welch's t -test. The underlying histograms are included in Figure S4 of the Supporting Information S1.

Across all tracked TCs, there are small, but statistically significant, increases in mean intensity with warming. The average (top 5%) MSLP drops by 1 hPa (6 hPa) and $u_{10m,x}$ increases by 1.5 m s^{-1} (3.8 m s^{-1}) between the historical and warmest “hot far” runs. This is consistent with PI theory, which suggests increasing TC intensity with increasing SSTs (Emanuel, 1986; Holland, 1997). Mean SST in a $5^\circ \times 5^\circ$ box under the TC center is also listed in Table 1. Normalizing $u_{10m,x}$ by under-TC SST changes yields estimates of $2.1\%–2.5\% \text{ }^\circ\text{C}^{-1}$, which is on par with, but slightly lower than, estimates from Knutson et al. (2015) ($2.9\% \text{ }^\circ\text{C}^{-1}$) and S. Wang and Toumi (2018) ($3\%–4\% \text{ }^\circ\text{C}^{-1}$) and slightly above that found in Nolan et al. (2007) ($2.0\% \text{ }^\circ\text{C}^{-1}$). For both MSLP and $u_{10m,x}$, the 95th percentile (very intense TCs) increases more rapidly with warming compared to the mean. This implies a preferential intensification of the most intense TCs, projected to occur in future climates due to further enhancement of already favorable (e.g., high SST, low shear) environments (e.g., Emanuel, 2013; Knutson et al., 2020). Note that since TGW is conditional, such environments, in a relative sense, persist in the counterfactual runs (i.e., if an environment for a specific TC was favorable in the historical record, it is also favorable in all simulations here; also see Figure S5 in Supporting Information S1). Integrated kinetic energy (IKE) of the 850-hPa wind field, which is the spatial integral of the wind magnitude squared (Powell & Reinhold, 2007), similarly increases monotonically with warming, although only significantly in the warmest runs.

Larger changes occur in the metrics associated with moisture. Both the mean and 95th percentiles of TC TPW_x and Prec_x increase monotonically with warming. Assuming a Clausius-Clapyron (CC) scaling of 7% precipitation increase per 1°C of warming, mean TPW_x scales near CC ($5.9\%–6.4\% \text{ }^\circ\text{C}^{-1}$) relative to domain-averaged WL and slightly higher ($8.5\%–9.5\% \text{ }^\circ\text{C}^{-1}$) relative to the $5^\circ \times 5^\circ$ under-TC-center SST (Tables S5 and S6 in Supporting Information S1). Prec_x increases greater than CC ($9.0\%–10.1\% \text{ }^\circ\text{C}^{-1}$ WL and $13.4\%–14.2\% \text{ }^\circ\text{C}^{-1}$ SST) for the average TC. This enhanced precipitation efficiency is consistent with increased storm intensity with warming, a subsequent strengthening of the TC secondary circulation, and increased moisture convergence (C.-C. Wang et al., 2015). This result is close to, but slightly above, the consensus estimate in Knutson et al. (2020). Scaling of the 95th percentile values is similar for TPW_x ($6.1\%–6.7\% \text{ }^\circ\text{C}^{-1}$ WL and $8.8\%–10.0\% \text{ }^\circ\text{C}^{-1}$ SST) and slightly lower (but still super-CC) for Prec_x ($7.2\%–8.0\% \text{ }^\circ\text{C}^{-1}$ WL and $10.2\%–11.7\% \text{ }^\circ\text{C}^{-1}$ SST). The snapshot-level areal coverage of precipitation rates greater than 10 mm hr^{-1} similarly increases monotonically with WL.

While there are clear signals in MSLP and $u_{10m,x}$, there is no statistically significant change in the overall outer size of the TC as by the radius at which the azimuthally averaged 850-hPa wind magnitude drops below 8 m s^{-1} (r_8). This metric is chosen because of its fidelity in reanalyses and climate data (Schenkel et al., 2018). Note that since IKE is a spatial integral dependent on wind magnitude, its relative response is essentially a combination of $u_{10m,x}$ and r_8 . Across all TCs, the radius of maximum wind (RMW) contracts by 5–8 km in all warming simulations. There is sparse literature on climate model RMW projections, likely owing to insufficient model resolution to resolve inner core processes, but this result supports prior findings (Chen et al., 2022; Kanada et al., 2013). This is also consistent with operational knowledge, where $u_{10m,x}$ and RMW are generally inversely correlated (Chavas & Lin, 2016). We do caution that the mean RMW is only approximately 10 times the grid spacing of the model so while we believe this result to be credible, it is likely near the edge of resolvability. The lack of change in the exterior extent of the wind field coupled with changes in the quantities in the TC inner core region imply changes in the radially averaged structure with warming rather than monotonic expansions or contractions of the overall wind field, consistent with past modeling studies (Gutmann et al., 2018; Knutson et al., 2015).

Lastly, we include a metric of the variation in TC intensity (measured by the absolute value of 6-hourly MSLP change, $|\text{dPSL}|$). There are statistically significant increases in this variation with increasing warming. This result is partly expected from the more intense TCs as measured by MSLP (more intense TCs have more “room” to intensify/decay) but also may result from large-scale environmental changes that modulate TC intensity.

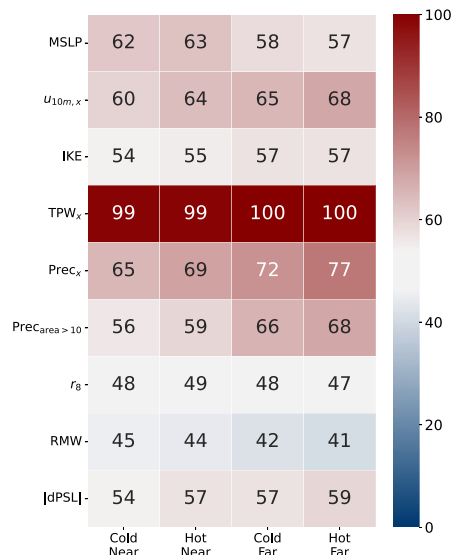


Figure 2. Percentage of TC snapshots for each metric (rows) and in each configuration (column) that increase relative to the historical control. Cells are color-coded by the magnitude of frequency change, with reds (blues) indicating increases (decreases). The sign of MSLP decrease frequency has been flipped to make it comparable to other intensity metrics.

3.2. Frequency of Directional Changes

While Table 1 shows changes in the bulk statistics, the TGW ensemble framework provides a unique way to evaluate the frequency with which storm quantities increase or decrease in the counterfactuals. That is because each snapshot in the historical simulation is paired one-to-one to a corresponding snapshot in the counterfactual runs (e.g., Figure 1's Hurricane Katrina at 12Z 29th August 2005 can be identically found in all five data sets). Figure 2 shows the frequency with which paired metrics increase in each of the counterfactual runs relative to the historical. For example, for $u_{10m,x}$, 64% of the TC snapshots in the “hot near” simulations increase relative to their matching counterpart TC in the historical simulation.

A few things are noteworthy. The fraction of storms that intensify in future climates, either as measured by $u_{10m,x}$ or MSLP, ranges from 57% to 68%. In other words, we find a large amount of variability in how historical TCs respond to imposed warming. 60% of snapshots show increased $u_{10m,x}$ in the “cold near” increasing to 68% in the “hot far.” MSLP is even more interesting, with the probability of a given snapshot becoming more intense actually decreasing for the “far” simulations compared to the “near” ones. This may be due to changes in the background SLP, as intensity is linked to the overall pressure gradient, not the absolute SLP minimum. IKE shows an even more muted response, with slightly better than a coin flip for increased intensity in “cold near” rising to 57% probability in “hot far.” Simply, increased warming does not lead to increased intensity in every synoptic setup.

In contrast, nearly every snapshot shows an increase in TPW_x with warming. There is greater than a 99% chance that a TC in the counterfactual simulations will be wetter from an environmental moisture perspective than its historical counterpart. However, $Prec_x$, which increases by a similar percentage amount to TPW_x in a mean sense (Table 1), only increases in 65%–77% of all storms in the counterfactuals depending on WL. We speculate that this is because maximum precipitation is a function of not only the background moisture content but also TC intensity. Therefore, the precipitation response is a combination of the responses from those metrics. Similar to the mean state changes, r_8 frequency increases are approximately 50% across all counterfactuals. TCs are just as likely to be larger as they are smaller in the counterfactuals; there is no obvious directional response in overall wind field extent, corroborating Schenkel et al. (2022). Chavas and Reed (2019) also theorize that temperature is not a key influencer of outer TC size. The frequency of RMW increase is below 50%, supporting the notion that the inner cores of TCs contract with warming. Finally, $|dPSL|$ preferentially increases in the warming runs (the 6-hourly swings in MSLP are larger with warming) with frequencies similar to the other dynamical intensity metrics.

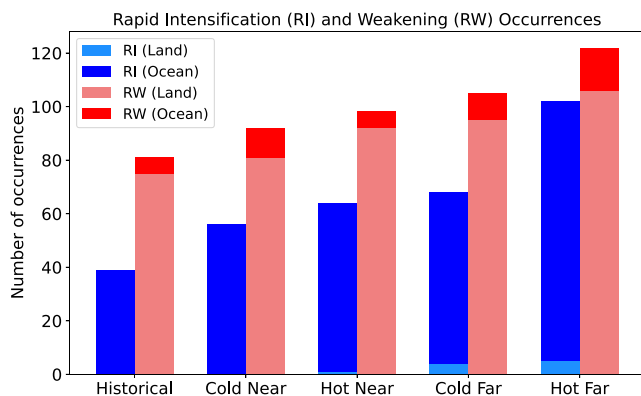


Figure 3. Total number of occurrences shown in blue (red) of RI (RW) defined by MSLP decreases (increases) greater than $7.5 \text{ hPa } 6\text{h}^{-1}$ in each simulation. Fractions of bars are shaded by whether the TC center at the end of the RI/RW period was over land or ocean.

3.3. Changes in Intensity Variability

To further explore the increased intensity variability, we investigate statistics of TCs that rapidly intensify and weaken. Rapid intensification (RI) is typically defined by changes in $u_{10m,x}$ (Kaplan & DeMaria, 2003). However, since models tend to simulate TC pressure better than wind (e.g., Hodges et al., 2017; C. M. Zarzycki et al., 2021) we define RI as 6-hourly periods where MSLP drops at least 7.5 hPa . This rate follows Peng et al. (2024) and is slightly below Holliday and Thompson (1979) ($10.5 \text{ hPa } 6\text{h}^{-1}$). Rapid weakening (RW) is defined similarly except for periods of pressure rises greater than $7.5 \text{ hPa } 6\text{h}^{-1}$.

Figure 3 shows a histogram of event occurrence, with the historical simulation on the left and increasing warming toward the right. There is a clear and marked increase for both RI and RW events with warming. The frequency of RI increases by approximately a factor of 2.5 between the historical and

warmest simulations. This implies increased intensity variability before landfall since TCs that undergo RI primarily do so over ocean surfaces (although a small fraction were flagged as RI over low-lying land in the warmer simulations). The RW results are a bit more complex since a storm may weaken quickly over ocean (e.g., in the presence of wind shear) but also can weaken expeditiously after landfall. Therefore, the increase in the RW events could mean more over-ocean variability during a TC's evolution but is also consistent with stronger storms at landfall, which have more "room" to undergo RW upon land surface interaction. Most RW events in our simulations are indeed associated with landfalling TCs, particularly over the northern Gulf Coast and mid-Atlantic regions (7% RW events occur over ocean vs. 93% over land). However, in the warmer simulations, additional instances of RW do occur offshore (13%), spatially concurrent with increases in near-coastal RI (Figure S6 in Supporting Information S1).

4. Discussion

We evaluate TCs in a 40-year historical reforecast and how they change in four counterfactual experiments with the same meteorology but different levels of warming. The 12 km WRF grid spacing permits intensities that are well-matched to observations and careful attention to tracking supports paired analysis of 4,498 TC/timestep combinations across all five simulations.

On average, storms become more intense regardless of whether measured by $u_{10m,x}$, MSLP, or IKE, with the tail of the intensity distribution skewing further toward stronger values as warming increases. Relative to these three metrics, moisture and precipitation quantities increase more strongly with warming. Mean TPW_x scales approximately with CC with $Prec_x$ scaling slightly above CC, which we speculate is due to stronger storms more efficiently converting vapor to precipitation. However, there is relatively large storm-to-storm variability, with some individual storms having decreased precipitation rates and others nearly doubling in the future. We find no consistent changes in outer storm size as measured by r_8 , although we find the average RMW contracts slightly inwards toward the storm center with warming. Increasing confidence in our findings, these results are broadly consistent with the CONUS TC changes in the TGW study of Gutmann et al. (2018).

A notable finding is the frequency of the directional response of various TC quantities across the paired samples. While the aforementioned aggregate responses across many TCs are consistent with previous modeling studies, our simulations indicate that these responses are highly variable for any particular storm. That is, it is far from a given that an individual TC will become stronger, or even wetter, in a TGW framework. The only metric that showed an extremely consistent response in nearly every snapshot was TPW_x —it is almost a virtual certainty that future TCs will have more available moisture than historical TCs. Both maximum rainfall rate and area of 10 mm hr^{-1} rainfall metrics increased more than they decreased, although even in the warmest simulations, snapshot maximum rainfall rates only increased in 77% of cases. These results have implications for single TC attribution studies (e.g., Lackmann, 2015; Reed et al., 2020) in that it should not be assumed all cases will or should conditionally increase in intensity (either as measured wind, pressure, or precipitation) in a warming climate. We acknowledge that we only have one realization of each TC snapshot in each of the five simulations and better characterizing uncertainty encourages applying perturbed ensembles in future studies.

Finally, intensity variability progressively increases in a warmed climate. This is apparent in the overall statistics, where the mean magnitude of the change in MSLP significantly increases in the counterfactuals. In a more extreme sense, this also includes both instances of RI and periods where a TC "falls apart," which predominantly occurs near or just after landfall. This finding aligns with previous studies both interrogating the historical record (S. Wang et al., 2020) and projecting increased RI frequency using statistical-dynamical downscaling (Emanuel, 2017). RI is considered one of the hardest challenges in TC forecasting (Judt et al., 2023); increasing RI frequency could further exacerbate this, particularly in coastal regions. However, we caution that 12 km simulations underresolve inner-core TC processes that may be important for RI (Davis et al., 2008). Future high-resolution storylines at kilometer-scale grid spacing may help further investigate this result.

Data Availability Statement

The raw data from the IM3/HyperFACETS thermodynamic global warming (TGW) simulations are described in Jones et al. (2023) and can be downloaded in Jones et al. (2022). TempestExtremes (Ullrich et al., 2021), used for tracking the TCs, extracting snapshots, and radially averaging wind fields, is open source and can be downloaded

at <https://github.com/ClimateGlobalChange/tempestextremes>. Processed NetCDF TC snapshots are archived at C. Zarzycki (2024a). All TC trajectories and code used in this manuscript with instructions to reproduce the results are at C. Zarzycki (2024b).

Acknowledgments

This work was supported by the US Department of Energy (DOE), Office of Science, Office of Biological and Environmental Research program under DE-SC0016605 “A framework for improving analysis and modeling of Earth system and sectoral dynamics at regional scales.” Work performed by PAU is in part supported by the US DOE at Lawrence Livermore National Laboratory under DE-AC52-07NA27344. Work performed by ADJ and PV is supported by the DOE under DE-AC02-05CH11231. This research used resources from the National Energy Research Scientific Computing Center (NERSC), a DOE facility located at Lawrence Berkeley National Laboratory (DE-AC02-05CH11231). DR is an employee of UT-Battelle, LLC, under DOE DEAC05-00OR22725. Accordingly, the publisher, by accepting the article for publication, acknowledges that the US government retains a nonexclusive, paid-up, irrevocable, worldwide license to publish or reproduce the published form of this manuscript or allow others to do so, for US government purposes. DOE will provide public access to these results of federally sponsored research in accordance with the DOE Public Access Plan (<https://www.energy.gov/downloads/doe-public-access-plan>).

References

- Balaguru, K., Foltz, G. R., Leung, L. R., & Emanuel, K. A. (2016). Global warming-induced upper-ocean freshening and the intensification of super typhoons. *Nature Communications*, 7(13670), 1–8. <https://doi.org/10.1038/ncomms13670>
- Bourdin, S., Fromang, S., Dulac, W., Cattiaux, J., & Chauvin, F. (2022). Intercomparison of four algorithms for detecting tropical cyclones using ERA5. *Geoscientific Model Development*, 15(17), 6759–6786. <https://doi.org/10.5194/gmd-15-6759-2022>
- Brogli, R., Heim, C., Mensch, J., Sørland, S. L., & Schär, C. (2023). The pseudo-global-warming (PGW) approach: Methodology, software package PGW4ERA5 v1.1, validation, and sensitivity analyses. *Geoscientific Model Development*, 16(3), 907–926. <https://doi.org/10.5194/gmd-16-907-2023>
- Chavas, D. R., & Lin, N. (2016). A model for the complete radial structure of the tropical cyclone wind field. Part II: Wind field variability. *Journal of the Atmospheric Sciences*, 73(8), 3093–3113. <https://doi.org/10.1175/JAS-D-15-0185.1>
- Chavas, D. R., & Reed, K. A. (2019). Dynamical aquaplanet experiments with uniform thermal forcing: System dynamics and implications for tropical cyclone genesis and size. *Journal of the Atmospheric Sciences*, 76(8), 2257–2274. <https://doi.org/10.1175/JAS-D-19-0001.1>
- Chen, J., Tam, C. Y., Wang, Z., Cheung, K., Li, Y., Lau, N.-C., & Lau, D.-S. D. (2022). Future thermodynamic impacts of global warming on landfalling typhoons and their induced storm surges to the Pearl River Delta Region as inferred from high-resolution regional models. *Journal of Climate*, 35(15), 4905–4926. <https://doi.org/10.1175/JCLI-D-21-0436.1>
- Chen, J., Wang, Z., Tam, C.-Y., Lau, N.-C., Lau, D.-S. D., & Mok, H.-Y. (2020). Impacts of climate change on tropical cyclones and induced storm surges in the Pearl River Delta region using pseudo-global-warming method. *Scientific Reports*, 10(1965), 1–10. <https://doi.org/10.1038/s41598-020-58824-8>
- Chow, T. N., Tam, C. Y., Chen, J., & Hu, C. (2024). Effects of background synoptic environment in controlling South China Sea tropical cyclone intensity and size changes in pseudo-global warming experiments. *Journal of Climate*, 37(5), 1811–1832. <https://doi.org/10.1175/JCLI-D-23-0503.1>
- Ciullo, A., Martius, O., Strobl, E., & Bresch, D. N. (2021). A framework for building climate storylines based on downward counterfactuals: The case of the European Union Solidarity fund. *Climate Risk Management*, 33, 100349. <https://doi.org/10.1016/j.crm.2021.100349>
- Davis, C. A. (2018). Resolving tropical cyclone intensity in models. *Geophysical Research Letters*, 45(4), 2082–2087. <https://doi.org/10.1002/2017GL076966>
- Davis, C. A., Wang, W., Chen, S. S., Chen, Y., Corbosiero, K., DeMaria, M., et al. (2008). Prediction of landfalling hurricanes with the advanced hurricane WRF model. *Monthly Weather Review*, 136(6), 1990–2005. <https://doi.org/10.1175/2007MWR2085.1>
- Delfino, R. J., Vidale, P. L., Bagtasa, G., & Hodges, K. (2023). Response of damaging Philippines tropical cyclones to a warming climate using the pseudo global warming approach. *Climate Dynamics*, 61(7), 3499–3523. <https://doi.org/10.1007/s00382-023-06742-6>
- Emanuel, K. A. (1986). An air-sea interaction theory for tropical cyclones. Part I: Steady-state maintenance. *Journal of the Atmospheric Sciences*, 43(6), 585–605. [https://doi.org/10.1175/1520-0469\(1986\)043<0585:AASITF>2.0.CO;2](https://doi.org/10.1175/1520-0469(1986)043<0585:AASITF>2.0.CO;2)
- Emanuel, K. A. (2013). Downscaling CMIP5 climate models shows increased tropical cyclone activity over the 21st century. *Proceedings of the National Academy of Sciences of the United States of America*, 110(30), 12219–12224. <https://doi.org/10.1073/pnas.1301293110>
- Emanuel, K. A. (2017). Will global warming make hurricane forecasting more difficult? *Bulletin of the American Meteorological Society*, 98(3), 495–501. <https://doi.org/10.1175/BAMS-D-16-0134.1>
- Gutmann, E. D., Rasmussen, R. M., Liu, C., Ikeda, K., Bruyere, C. L., Done, J. M., et al. (2018). Changes in hurricanes from a 13-yr convection-permitting pseudo-global warming simulation. *Journal of Climate*, 31(9), 3643–3657. <https://doi.org/10.1175/JCLI-D-17-0391.1>
- Haarsma, R. J., Roberts, M. J., Vidale, P. L., Senior, C. A., Bellucci, A., Bao, Q., et al. (2016). High Resolution Model Intercomparison Project (HighResMIP v1.0) for CMIP6. *Geoscientific Model Development*, 9(11), 4185–4208. <https://doi.org/10.5194/gmd-9-4185-2016>
- Hodges, K., Cobb, A., & Vidale, P. L. (2017). How well are tropical cyclones represented in reanalysis datasets? *Journal of Climate*, 30(14), 5243–5264. <https://doi.org/10.1175/JCLI-D-16-0557.1>
- Holland, G. J. (1997). The maximum potential intensity of tropical cyclones. *Journal of the Atmospheric Sciences*, 54(21), 2519–2541. [https://doi.org/10.1175/1520-0469\(1997\)054<2519:TMPLOT>2.0.CO;2](https://doi.org/10.1175/1520-0469(1997)054<2519:TMPLOT>2.0.CO;2)
- Holliday, C. R., & Thompson, A. H. (1979). Climatological characteristics of rapidly intensifying typhoons. *Monthly Weather Review*, 107(8), 1022–1034. [https://doi.org/10.1175/1520-0493\(1979\)107<1022:CCORIT>2.0.CO;2](https://doi.org/10.1175/1520-0493(1979)107<1022:CCORIT>2.0.CO;2)
- Huang, P., Lin, I.-I., Chou, C., & Huang, R.-H. (2015). Change in ocean subsurface environment to suppress tropical cyclone intensification under global warming. *Nature Communications*, 6(7188), 1–9. <https://doi.org/10.1038/ncomms8188>
- James, R., Washington, R., Schleussner, C.-F., Rogelj, J., & Conway, D. (2017). Characterizing half-a-degree difference: A review of methods for identifying regional climate responses to global warming targets. *WIREs Climate Change*, 8(2), e457. <https://doi.org/10.1002/wcc.457>
- Jones, A. D., Rastogi, D., Vahmani, P., Stansfield, A., Reed, K., Thurber, T., et al. (2022). IM3/HyperFACETS thermodynamic global warming (TGW) simulation datasets: v1.0.0 [Dataset]. *MSD-LIVE Data Repository*. <https://doi.org/10.57931/1885756>
- Jones, A. D., Rastogi, D., Vahmani, P., Stansfield, A. M., Reed, K. A., Thurber, T., et al. (2023). Continental United States climate projections based on thermodynamic modification of historical weather. *Scientific Data*, 10(664), 1–21. <https://doi.org/10.1038/s41597-023-02485-5>
- Judt, F., Rios-Berrios, R., & Bryan, G. H. (2023). Marathon versus sprint: Two modes of tropical cyclone rapid intensification in a global convection-permitting simulation. *Monthly Weather Review*, 151(10), 2683–2699. <https://doi.org/10.1175/MWR-D-23-0038.1>
- Kanada, S., Wada, A., & Sugi, M. (2013). Future changes in structures of extremely intense tropical cyclones using a 2-km mesh nonhydrostatic model. *Journal of Climate*, 26(24), 9986–10005. <https://doi.org/10.1175/JCLI-D-12-00477.1>
- Kaplan, J., & DeMaria, M. (2003). Large-scale characteristics of rapidly intensifying tropical cyclones in the North Atlantic basin. *Weather and Forecasting*, 18(6), 1093–1108. [https://doi.org/10.1175/1520-0434\(2003\)018<1093:LCORIT>2.0.CO;2](https://doi.org/10.1175/1520-0434(2003)018<1093:LCORIT>2.0.CO;2)
- Knapp, K. R., Kruk, M. C., Levinson, D. H., Diamond, H. J., & Neumann, C. J. (2010). The international best track archive for climate stewardship (IBTrACS). *Bulletin of the American Meteorological Society*, 91(3), 363–376. <https://doi.org/10.1175/2009BAMS2755.1>
- Knutson, T., Camargo, S. J., Chan, J. C. L., Emanuel, K., Ho, C.-H., Kossin, J., et al. (2020). Tropical cyclones and climate change assessment: Part II: Projected response to anthropogenic warming. *Bulletin of the American Meteorological Society*, 101(3), E303–E322. <https://doi.org/10.1175/BAMS-D-18-0194.1>

- Knutson, T., Sirutis, J. J., Zhao, M., Tuleya, R. E., Bender, M., Vecchi, G. A., et al. (2015). Global projections of intense tropical cyclone activity for the late twenty-first century from dynamical downscaling of CMIP5/RCP4.5 scenarios. *Journal of Climate*, 28(18), 7203–7224. <https://doi.org/10.1175/JCLI-D-15-0129.1>
- Lackmann, G. M. (2015). Hurricane Sandy before 1900 and after 2100. *Bulletin of the American Meteorological Society*, 96(4), 547–560. <https://doi.org/10.1175/BAMS-D-14-00123.1>
- Meinshausen, M., Nicholls, Z. R. J., Lewis, J., Gidden, M. J., Vogel, E., Freund, M., et al. (2020). The shared socio-economic pathway (SSP) greenhouse gas concentrations and their extensions to 2500. *Geoscientific Model Development*, 13(8), 3571–3605. <https://doi.org/10.5194/gmd-13-3571-2020>
- Mendelsohn, R., Emanuel, K., Chonabayashi, S., & Bakkensen, L. (2012). The impact of climate change on global tropical cyclone damage. *Nature Climate Change*, 2(3), 205–209. <https://doi.org/10.1038/nclimate1357>
- Nolan, D. S., Rappin, E. D., & Emanuel, K. A. (2007). Tropical cyclogenesis sensitivity to environmental parameters in radiative-convective equilibrium. *Quarterly Journal of the Royal Meteorological Society*, 133(629), 2085–2107. <https://doi.org/10.1002/qj.170>
- Olschewski, P., & Kunstmann, H. (2024). Future projections of hurricane intensity in the southeastern U.S.: Sensitivity to different pseudo-global warming methods. *Frontiers in Climate*, 6, 1353396. <https://doi.org/10.3389/fclim.2024.1353396>
- Parker, C. L., Bruyère, C. L., Mooney, P. A., & Lynch, A. H. (2018). The response of land-falling tropical cyclone characteristics to projected climate change in northeast Australia. *Climate Dynamics*, 51(9), 3467–3485. <https://doi.org/10.1007/s00382-018-4091-9>
- Parker, W. S. (2011). When climate models agree: The significance of robust model predictions. *Philosophy of Science*, 78(4), 579–600. <https://doi.org/10.1086/661566>
- Patricola, C. M., & Wehner, M. F. (2018). Anthropogenic influences on major tropical cyclone events. *Nature*, 563(7731), 339–346. <https://doi.org/10.1038/s41586-018-0673-2>
- Peng, K., Tian, Y.-X., Fang, J., Liu, Y., & Gu, J.-F. (2024). Diversity of tropical cyclones rapid intensification. *Geophysical Research Letters*, 51(13), e2023GL108006. <https://doi.org/10.1029/2023GL108006>
- Powell, M. D., & Reinhold, T. A. (2007). Tropical cyclone destructive potential by integrated kinetic energy. *Bulletin of the American Meteorological Society*, 88(4), 513–526. <https://doi.org/10.1175/BAMS-88-4-513>
- Reddy, P. J., Sriram, D., Gunthe, S. S., & Balaji, C. (2021). Impact of climate change on intense Bay of Bengal tropical cyclones of the post-monsoon season: A pseudo global warming approach. *Climate Dynamics*, 56(9), 2855–2879. <https://doi.org/10.1007/s00382-020-05618-3>
- Reed, K. A., Stansfield, A. M., Wehner, M. F., & Zarzycki, C. M. (2020). Forecasted attribution of the human influence on Hurricane Florence. *Science Advances*, 6(1). <https://doi.org/10.1126/sciadv.aaw9253>
- Roberts, M. J., Camp, J., Seddon, J., Vidale, P. L., Hodges, K., Vanniere, B., et al. (2020). Impact of model resolution on tropical cyclone simulation using the HighResMIP-PRIMAVERA multimodel ensemble. *Journal of Climate*, 33(7), 2557–2583. <https://doi.org/10.1175/JCLI-D-19-0639.1>
- Schär, C., Frei, C., Lüthi, D., & Davies, H. C. (1996). Surrogate climate-change scenarios for regional climate models. *Geophysical Research Letters*, 23(6), 669–672. <https://doi.org/10.1029/96GL00265>
- Schenkel, B. A., Chavas, D., Lin, N., Knutson, T., Vecchi, G., & Brammer, A. (2022). North Atlantic tropical cyclone outer size and structure remain unchanged by the late twenty-first century. *Journal of Climate*, 36(2), 359–382. <https://doi.org/10.1175/JCLI-D-22-0066.1>
- Schenkel, B. A., Lin, N., Chavas, D., Vecchi, G. A., Oppenheimer, M., & Brammer, A. (2018). Lifetime evolution of outer tropical cyclone size and structure as diagnosed from reanalysis and climate model data. *Journal of Climate*, 31(19), 7985–8004. <https://doi.org/10.1175/JCLI-D-17-0630.1>
- Shepherd, T. G., Boyd, E., Calel, R. A., Chapman, S. C., Dessai, S., Dima-West, I. M., et al. (2018). Storylines: An alternative approach to representing uncertainty in physical aspects of climate change. *Climatic Change*, 151(3), 555–571. <https://doi.org/10.1007/s10584-018-2317-9>
- Tran, T. L., Ritchie, E. A., Perkins-Kirkpatrick, S. E., Bui, H., & Luong, T. M. (2022). Future changes in tropical cyclone exposure and impacts in southeast Asia from CMIP6 pseudo-global warming simulations. *Earth's Future*, 10(12), e2022EF003118. <https://doi.org/10.1029/2022EF003118>
- Ullrich, P. A., & Zarzycki, C. M. (2017). TempestExtremes: A framework for scale-insensitive pointwise feature tracking on unstructured grids. *Geoscientific Model Development*, 10(3), 1069–1090. <https://doi.org/10.5194/gmd-10-1069-2017>
- Ullrich, P. A., Zarzycki, C. M., McClenny, E. E., Pinheiro, M. C., Stansfield, A. M., & Reed, K. A. (2021). TempestExtremes v2.1: A community framework for feature detection, tracking, and analysis in large datasets. *Geoscientific Model Development*, 14(8), 5023–5048. <https://doi.org/10.5194/gmd-14-5023-2021>
- Wang, C.-C., Lin, B.-X., Chen, C.-T., & Lo, S.-H. (2015). Quantifying the effects of long-term climate change on tropical cyclone rainfall using a cloud-resolving model: Examples of two landfall typhoons in Taiwan. *Journal of Climate*, 28(1), 66–85. <https://doi.org/10.1175/JCLI-D-14-00044.1>
- Wang, S., Rashid, T., Throp, H., & Toumi, R. (2020). A shortening of the life cycle of major tropical cyclones. *Geophysical Research Letters*, 47(14), e2020GL088589. <https://doi.org/10.1029/2020GL088589>
- Wang, S., & Toumi, R. (2018). Reduced sensitivity of tropical cyclone intensity and size to sea surface temperature in a radiative-convective equilibrium environment. *Advances in Atmospheric Sciences*, 35(8), 981–993. <https://doi.org/10.1007/s00376-018-7277-5>
- Wehner, M. F., Zarzycki, C., & Patricola, C. (2019). Estimating the human influence on tropical cyclone intensity as the climate changes. In *Hurricane Risk* (pp. 235–260). Springer.
- Zarzycki, C. (2024a). Changes in four decades of near-CONUS tropical cyclones in an ensemble of 12km thermodynamic global warming simulations [Dataset]. *Zenodo*. <https://doi.org/10.5281/zenodo.11453972>
- Zarzycki, C. (2024b). zarzycki/tgw-tc: v1.0 [Software]. *Zenodo*. <https://doi.org/10.5281/zenodo.13272321>
- Zarzycki, C. M., Ullrich, P. A., & Reed, K. A. (2021). Metrics for evaluating tropical cyclones in climate data. *Journal of Applied Meteorology and Climatology*, 60(5), 643–660. <https://doi.org/10.1175/JAMC-D-20-0149.1>

References From the Supporting Information

- Franklin, J. L., Black, M. L., & Valde, K. (2000). Eyewall wind profiles in hurricanes determined by GPS dropwindsondes. In *Preprints, 24th conference on hurricanes and tropical meteorology, Fort Lauderdale, FL*. American Meteorological Society.
- Kreussler, P., Caron, L.-P., Wild, S., Tomas, S. L., Chauvin, F., Moine, M.-P., et al. (2021). Tropical cyclone integrated kinetic energy in an ensemble of HighResMIP simulations. *Geophysical Research Letters*, 48(5), e2020GL090963. <https://doi.org/10.1029/2020GL090963>

- Manganello, J. V., Hodges, K. I., Dirmeyer, B., Kinter, J. L., Cash, B. A., Marx, L., et al. (2014). Future changes in the western North Pacific tropical cyclone activity projected by a multidecadal simulation with a 16-km global atmospheric GCM. *Journal of Climate*, 27(20), 7622–7646. <https://doi.org/10.1175/jcli-d-13-00678.1>
- Murakami, H., & Sugi, M. (2010). Effect of model resolution on tropical cyclone climate projections. *Sola*, 6, 73–76. <https://doi.org/10.2151/sola.2010-019>